

1 *STH-net*: a ~~model-driven~~ soil monitoring network for process-based 2 hydrological modelling from the pedon to the hillslope scale

3 Edoardo Martini^{1,2}, [Matteo Bauckholt](#)², Simon Kögler^{3a}, Manuel Kreck², Kurt Roth¹, Ulrike Werban²,
4 Ute Wollschläger^{3,4}, Steffen Zacharias²

5 ¹ Institute of Environmental Physics, Heidelberg University, Heidelberg, 69120, Germany

6 ² Dept. Monitoring and Exploration Technologies, Helmholtz Centre for Environmental Research GmbH - UFZ, Leipzig,
7 04318, Germany

8 ^{3-a} formerly at: Dept. Monitoring and Exploration Technologies, Helmholtz Centre for Environmental Research GmbH - UFZ,
9 Leipzig, 04318, Germany

10 ⁴⁻³ Dept. Soil System Science, Helmholtz Centre for Environmental Research GmbH - UFZ, Halle (Saale), 06120, Germany

11 Correspondence to: Edoardo Martini (emartini@iup.uni-heidelberg.de)

12 **Abstract.** The *Schäfertal hillslope* site is part of the TERENO Harz/Central German Lowland Observatory and its soil water
13 dynamics ~~is~~are being monitored intensively as part of an integrated, long-term, multi-scale and multi-temporal research
14 framework linking hydrological, pedological, atmospheric and biodiversity-related research to investigate the influences of
15 climate and land use change on the terrestrial system. Here, a new soil monitoring network, indicated as *STH-net*, has been
16 recently implemented to provide high-resolution data about the most relevant hydrological variables and local soil properties.
17 The monitoring network is spatially optimized, based on previous knowledge from soil mapping and soil moisture monitoring,
18 in order to capture the spatial variability of soil properties and soil water dynamics along a catena across the site as well as in
19 depth. The *STH-net* comprises eight stations instrumented with time-domain reflectometry (TDR) probes, soil temperature
20 probes and ~~piezometers~~monitoring wells. Furthermore, a weather station provides data about the meteorological variables. A
21 detailed soil characterization exists for locations where the TDR probes are installed. All data are measured at a 10-minutes
22 interval since January 1st, 2019. The *STH-net* is intended to provide scientists with ~~high-quality~~ data needed for developing
23 and testing modelling approaches in the context of vadose-zone hydrology at spatial scales ranging from the pedon to the
24 hillslope. The data are available from the EUDAT portal
25 (~~<https://b2share.eudat.eu/records/e2a2135bb1634a97abcedf8a461e0909>~~[https://b2share.eudat.eu/records/82818db7be054f5eb](https://b2share.eudat.eu/records/82818db7be054f5eb921d386a0bcaa74)
26 [921d386a0bcaa74](https://b2share.eudat.eu/records/82818db7be054f5eb921d386a0bcaa74)) (Martini et al., 2020).

27 **1 Introduction**

28 Soils are embedded in the ~~larger~~ environment, coupled to vegetation and atmosphere at the land surface and to groundwater at
29 its lower end. This coupling gives rise to a suite of physical, chemical, and biological dynamics most of which are highly non-
30 linear and varying in time and space. Soils provide crucial ecosystem functions such as water storage and filtering, food and
31 other biomass production, recycling of carbon and nutrients, biological habitat and gene pool, ~~as well as~~ physical and cultural
32 heritage, source of raw materials and platforms for human life (United Nations, 2014; Vereecken et al., 2016). Soils are widely
33 distributed on the Earth surface. [Flow and transport processes in unsaturated soils occur predominantly in the vertical](#)

34 direction, with the gravity force playing a major role~~but the strongest gradients in soil systems occur in the vertical direction,~~
35 as abrupt changes in soil properties due to soil horizons and layers are typically more significant than those in the lateral
36 direction, and because of the strong coupling between soil, vegetation, and atmosphere. Therefore, despite the relevance of
37 soils for global phenomena, the relevant soil processes are rather local. Here, one aspect that complicates the picture is the
38 heterogeneity of ~~the soil properties, as soils are heterogeneous at all spatial scales.~~ Another one is the non-linearity of soil
39 processes. In order to address effectively this complexity, state-of-the-art experimental approaches must be coupled to,~~hence~~
40 numerical models ~~are needed~~ for the comprehensive representation of the system properties, states and ~~estimation of the~~ fluxes
41 ~~towards an improved understanding of~~ so that the hydrological system can be better understood.

42 Recently, Vogel (2019) provided a comprehensive discussion about the scales and scaling issues in the context of soil
43 hydrological research and ~~remarked~~ noted the need for looking at small-scale soil properties (i.e., at the pedon scale, at which
44 soil physics is capable of describing states and fluxes with sufficient accuracy) as a necessary step towards understanding and
45 summarizing the processes at larger scales. In this respect, the author stresses the need for a two-steps approach based on the
46 accurate description of the soil water dynamics at the pedon scale and accounting for the spatial patterns of functional soil types
47 that constitute the landscape, including the vertical stratification of soil hydraulic properties and structural attributes. However,
48 the author remarks that ~~, with the landscape being the typical scale of application of hydrological research at which, however,~~
49 high-resolution measurements of the relevant states and properties cannot be achieved at the larger scale (i.e., catchment, the
50 typical scale of application of hydrological research). In this context, the intermediate scale of hillslopes is crucial for linking
51 the detailed process understanding to larger scale dynamics, recognizing hillslopes as key landscape features that organize
52 water availability on land (Fan et al., 2019). ~~Hypotheses testing and falsification in vadose zone hydrology can be facilitated~~
53 ~~if observations are merged with models that honour the relevant nonlinear interactions.~~ In this respect, coupling state of the art
54 hydrological modelling approaches with high-resolution subsurface characterization can lead to an accurate quantification of
55 the soil water dynamics in the vadose zone (Vereecken et al., 2015).

56 The physical description of the small-scale water movement through the soil's porous structure is typically achieved using the
57 Richards equation. However, the detailed description of the material properties is needed and cannot be fully resolved by direct
58 sampling. Thus, inverse modelling can be a powerful tool for the estimation of the soil hydraulic parameters (e.g., Vrugt et al.,
59 2008), including the recent developments in data assimilation approaches (e.g., Bauser et al., 2016, 2020; Botto et al., 2018).
60 These require dense (in the direction of the dominant flow, typically orthogonal to the soil surface) measurements of soil water
61 content with high temporal resolution and of high quality. Furthermore, *in situ* sensors can experience all the processes
62 affecting the measured state variables in their natural environment (Wollschläger et al., 2009), which is an important advantage
63 with respect to sample-based determinations from the laboratory.

64 The performances of hydrological models can be improved by various measured data with high spatial and temporal resolution
65 (Clark et al., 2017). Bronstert (1999) ~~remarked~~ highlighted the importance of linking experimental knowledge to the experience
66 gained from numerical modelling applications as a very valuable synergistic combination. Technological advances in our
67 ability to measure soil hydrological states efficiently at the hillslope scale and beyond are one possible way to gain the much-

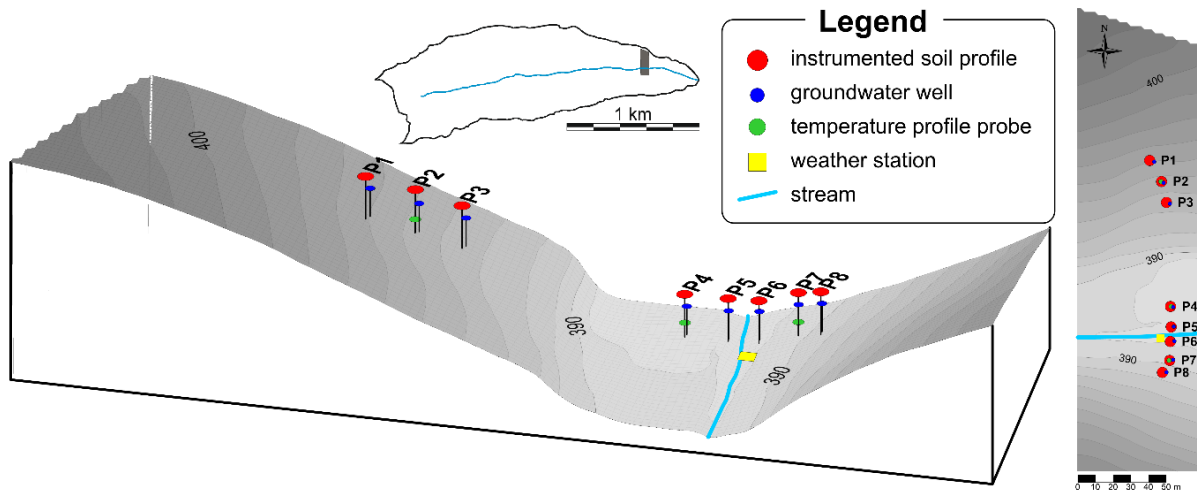
68 needed improved understanding of processes that challenge the comprehensive understanding of field-scale hydrology. ~~Critical~~
69 ~~Zone Observatories (e.g., Brantley et al., 2007; Anderson et al., 2008; White et al., 2015), environmental research platforms~~
70 ~~focusing on the interconnection between physical, chemical and biological processes affecting Earth surface, offer the~~
71 ~~opportunity to integrate information about different compartments of the environment, scales, and knowledge from different~~
72 ~~disciplines, which can potentially lead to the enhanced understanding of soil processes (e.g., Guo and Lin, 2016).~~
73 In the research framework of the TERENO Harz/Central German Lowland Observatory, the *Schäfertal hillslope* represents a
74 benchmark site for developing and testing the integration of state-of-the-art monitoring techniques with advanced modelling
75 approaches. This offers the opportunity to gain a more detailed understanding of processes and to quantify and predict water
76 and matter fluxes at nested spatial scales in the context of climate and land use change. Specifically, the approach followed at
77 the site accounts for the soil spatial variability through detailed soil mapping and is designed to provide *in situ* data ~~of, to our~~
78 ~~knowledge, the best quality available to date,~~ with high temporal resolution and dense coverage in the vertical direction, about
79 the soil water dynamics in the vadose zone and of its boundary conditions. With this design tailored to the needs of vadose
80 zone modelling, we aim ~~at feeding to provide~~ physical models with ideally all the data needed for quantifying and predicting
81 the soil water fluxes at spatial scales ranging from the pedon to the hillslope scale, with important implications, in terms of
82 methodological advance and process understanding, for catchment-scale processes.

83 Here, we present the first 21 months of the comprehensive dataset measured by the monitoring network *STH-net*, recently
84 implemented at *Schäfertal Hillslope* site, part of an intensive hydrological observatory. The data set includes hourly time series
85 of the meteorological forcing, soil water content measured *in situ* at different locations and at multiple soil depths along a
86 hillslope transect, soil physical and physicochemical properties.

87 **2 Site description**

88 The Schäfertal experimental site is a small headwater catchment (1.44 km²) located in the Lower Harz Mountains, in Central
89 Germany (51°39' N, 11°3' E). Environmental research at the Schäfertal catchment was initiated at the end of the 1960s with
90 the implementation of a hydro-meteorological station (Reinstorf et al., 2010) and the infrastructure has continuously been
91 expanded since then. Since 2010, the Schäfertal catchment is one of the highly instrumented intensive research sites within the
92 TERENO Harz/Central German Lowland Observatory (Zacharias et al., 2011, Wollschläger et al., ~~2018~~2017). Due to the
93 geographical settings of the Harz region, the Schäfertal catchment receives only 630 mm of precipitation per year. The average
94 annual air temperature is 6.9°C, with a sub-continental ~~superimposed on the~~ climate (Reinstorf, 2010). The geology of the
95 catchment is dominated by Devonian argillaceous shales and greywackes, covered by periglacial sediments (Borchardt, 1982).
96 Near-surface compacted horizons within the basal layer are known to induce interflow processes in the unsaturated zone
97 (Borchardt, 1982; Gräff et al., 2009). Dominant soil types in the Schäfertal are Gleysols occurring in the valley bottom as well
98 as Luvisols and Cambisols on the loess-covered slopes (Ollesch et al., 2005). The slopes of the catchment are intensively used
99 for agriculture, whilst meadows ~~occupies occupy~~ the valley bottom (Schröter et al., 2015).

100 Since 2012, a smaller hillslope area named *Schäfertal Hillslope* site, located downstream of the Schäfertal gauging station,
 101 was instrumented for detailed investigations of the hydrological processes in the unsaturated zone. From 2012 to 2017, the
 102 wireless soil moisture monitoring network *SoilNet* has delivered information about the soil water dynamics at three depths
 103 within the unsaturated zone with high spatial coverage. In 2018, the *SoilNet* has been disposed and a new soil monitoring
 104 network, named *STH-net*, has been installed aiming to improve the resolution in the vertical direction at a fewer locations
 105 selected based on the knowledge about the soil spatial variability and soil water dynamics gained from the previous monitoring
 106 experience (see Martini et al., 2015; 2017a; 2017b). The *STH-net* is described in the following sections of this manuscript and
 107 its data are now available through the data portal EUDAT
 108 (<https://b2share.eudat.eu/records/82818db7be054f5eb921d386a0bcaa74>). The *Schäfertal Hillslope* site includes north- and
 109 south-exposed slopes divided by the creek (*Schäferbach*) in the valley bottom (Fig. 1). In contrast to the slopes upstream-of
 110 the gauging station, which are primarily covered by cropland, this grassland transect is used as pasture and is not affected by
 111 agricultural practices except that the grass is mowed typically once per year. The spatial extent of the hillslope is approximately
 112 250 by 80 m and presents various topographical and pedological features. [The slopes are covered by silty loam Cambisols
 113 more evolved towards the footslope, while loam and silty loam stagnic Gleysols occupy the valley bottom. An extensive
 114 description of the soil units mapped at the site is provided in Martini et al. \(2015\).](#) The *STH-net* is designed to cover the spatial
 115 variability of the soil properties as well as the soil layering with high resolution.



116

117 **Figure 1: Spatial map in 3D and aerial view of the *Schäfertal hillslope* site and location of the monitoring stations.**

118 **3 Monitoring design and measurement techniques**

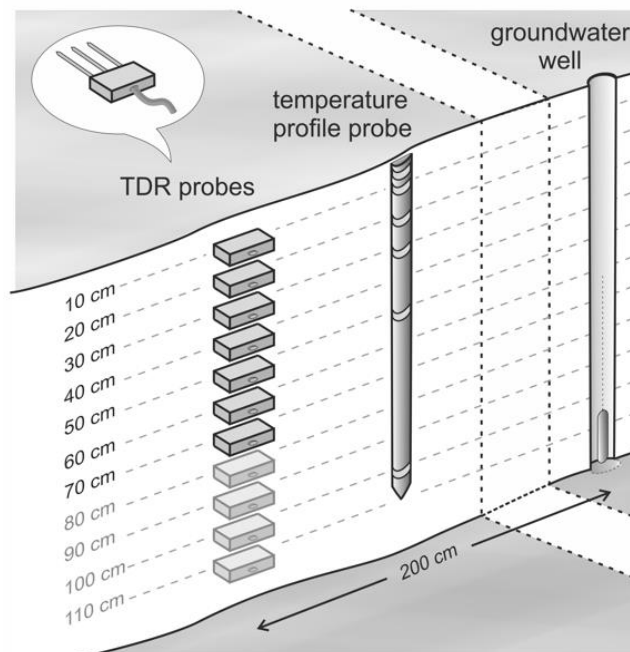
119 The *STH-net* comprises eight monitoring stations (named as P1 to P8) arranged along a transect centred within the *Schäfertal*
 120 *Hillslope* site and aligned along the slope direction (Fig.1). The stations P1, P2 and P3 are located within the Northern (i.e.,

121 South-facing) slope and cover the transition between the soil units STU1 and STU2 described in Martini et al. (2015); the
122 stations P4 and P5 fall into the valley bottom, i.e., soil unit STU3; P6, P7 and P8 cover the lower part of the Southern (i.e.,
123 North-facing) slope, i.e., soil unit STU4. Every station features a soil profile instrumented with Time-Domain Reflectometry
124 (TDR) probes installed every 0.1 m along the vertical direction. A sketch showing the design of a reference monitoring station
125 is presented in Fig. 2. Each of the instrumented soil profiles located on the hillslopes features a minimum of seven TDR probes
126 installed at the depths of 0.1, 0.2, 0.3, 0.4, 0.5, 0.6 and 0.7 m, whilst an additional probe is installed at P3 at the depth of 0.8 m
127 and the profiles at P4 and P5 feature additional TDR probes at the depths of 0.8, 0.9, 1.0 and 1.1 m in order to cover the deeper
128 soils. In a few cases, the depths of the probes were adjusted to avoid installing the TDR probe at or too close to the boundaries
129 between soil horizons. The exact depth of every TDR probe is reported in the file “STH-net_Soils.txt” and displayed in Fig.
130 3.

131 At every station, a well instrumented with a piezometer for monitoring the groundwater level was installed ca. 2 m to the East
132 of the instrumented soil profiles for monitoring the water level. One station for every topographic unit (i.e., Northern slope,
133 valley bottom and Southern slope) was further instrumented with sensors measuring the soil temperature at six depths between
134 0.05 and 1.0 m.

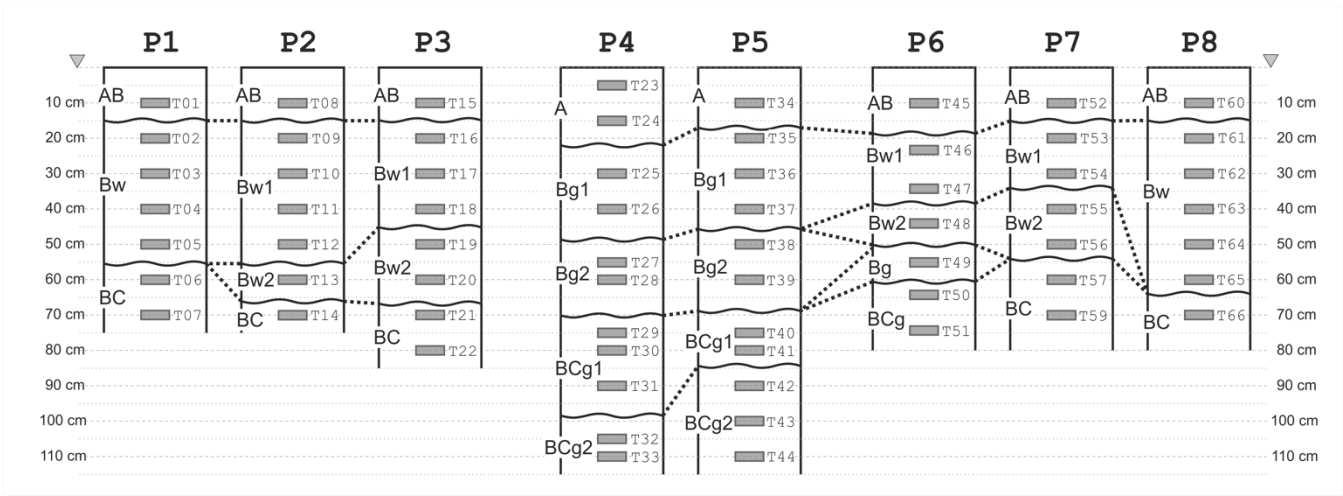
135 A weather station is located in the centre of the hillslope transect next to the creek.

136 All measurement systems comprising the *STH-net* collect measurements every 10 minutes, with the only exception of the
137 water level data which are collected every 2 hours.



138

139 **Figure 2: Sketch of a representative monitoring station of the *STH-net*.**



140

141 **Figure 3: Sketch of the soil profiles ([showing the mapped soil horizons according to WRB 2015](#)) and the depth of the TDR probes**
 142 **(see labels).**

143 3.1 TDR measurements

144 The TDR probes are arranged in clusters of 22 probes for the Northern slope and the valley bottom, whilst only 21 probes were
 145 installed at the Southern slope, for a total of 65 TDR probes. Each cluster consists of one TDR device (TDR100 for the station
 146 North, TDR200 for the stations Valley and South, Campbell Scientific Inc., Logan, UT, United States) and a data logger
 147 (CR1000 for the station North, CR6 for the stations Valley and South, Campbell Scientific Inc., Logan, UT, United States).
 148 The clusters are powered by ~~safety~~ extra low voltage cables buried ca. 0.3 m below the ground and cased in HDPE (i.e., high-
 149 density polyethylene) tubes and an AGM (i.e., absorbent glass mat) battery capable of supplying the required power in case of
 150 power cut-off. Every TDR probe is connected to its station master by a 22-m long low loss coaxial cable, tested to be the
 151 optimal length providing good signal quality while enabling enough flexibility in terms of network design. The TDR probes
 152 [were custom made and](#) have three 0.2 m-long rods. [They](#) were ~~self produced and~~ calibrated through measurements in air and
 153 in water with different salt concentrations for water content and electrical conductivity estimation. The probes were installed
 154 horizontally in soil pits which were carefully refilled after the installation. The installation was carried out between June and
 155 August 2018 and all the measurements collected until the end of December 2018 were discarded to allow the soil to re-compact
 156 naturally during the first rainy season.

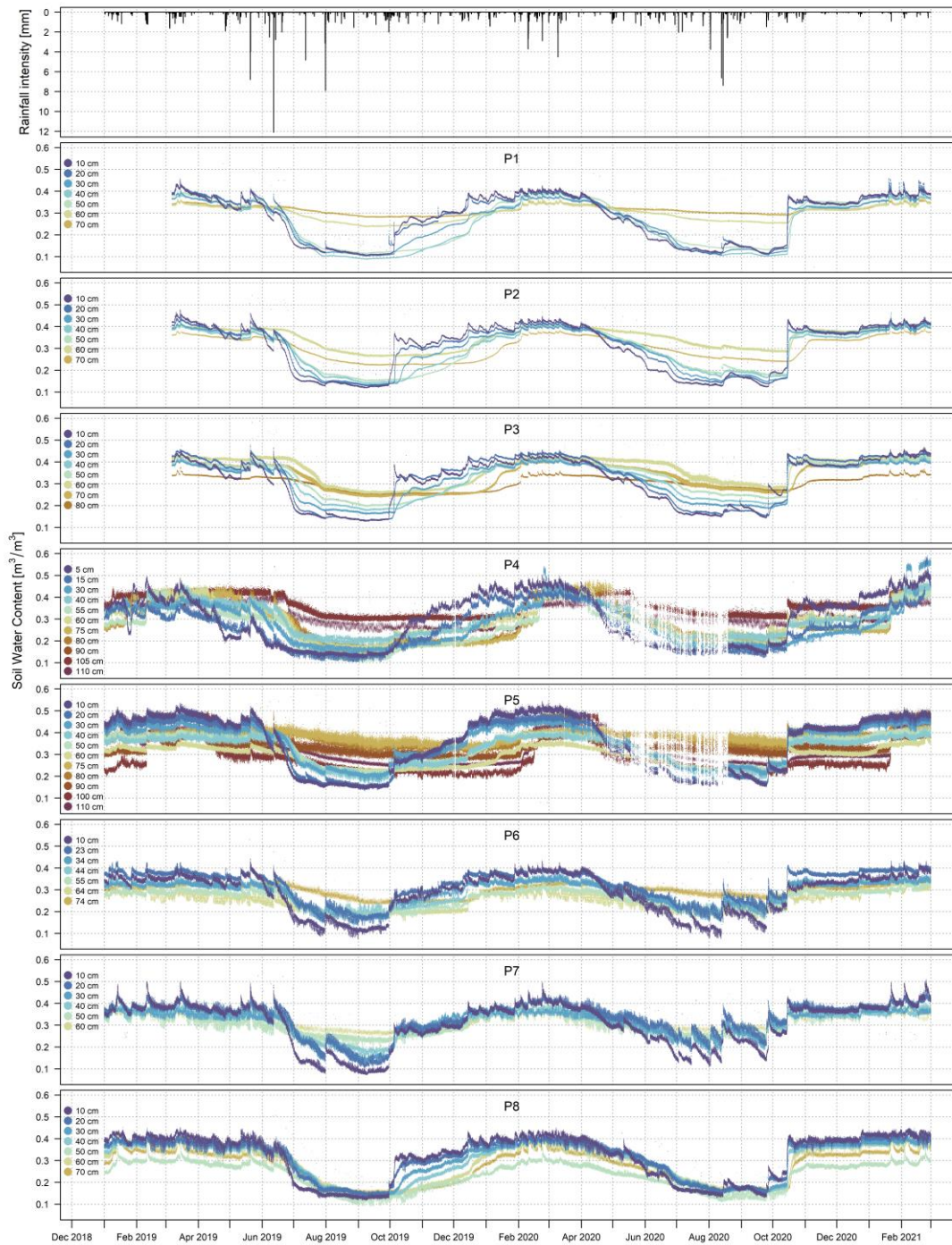
157 From the TDR traces, the dielectric permittivity ϵ of the medium is calculated as:

$$\sqrt{\epsilon} = \frac{(\sqrt{\epsilon_{air}} - \sqrt{\epsilon_{water}})(t - t_{water})}{t_{air} - t_{water}} + \sqrt{\epsilon_{air}} \quad (1)$$

158 based on the calibration measurements of travel time and dielectric permittivity in air (t_{air} , ϵ_{air}) and water (t_{water} , ϵ_{water}), where
 159 t is the travel time estimated for the measured trace. The volumetric water content θ is calculated according to the complex
 160 refractive index model (CRIM) following Roth et al. (1990) as:

$$\theta = \frac{\sqrt{\varepsilon} - \sqrt{\varepsilon_{soil}} - \phi(\sqrt{\varepsilon_{air}} - \sqrt{\varepsilon_{soil}})}{\sqrt{\varepsilon_{water}} - \sqrt{\varepsilon_{air}}} \quad (2)$$

161 where ϕ is the porosity which was calculated from the soil bulk density and ε_{soil} is set to 4.6. Fig. 4 shows the hourly time
162 series of soil water content. Characteristic differences in the soil water dynamics are evident for the distinct soil profiles and
163 depths to be attributed, e.g., to the differences in soil texture and soil layering or, locally to groundwater dynamics.

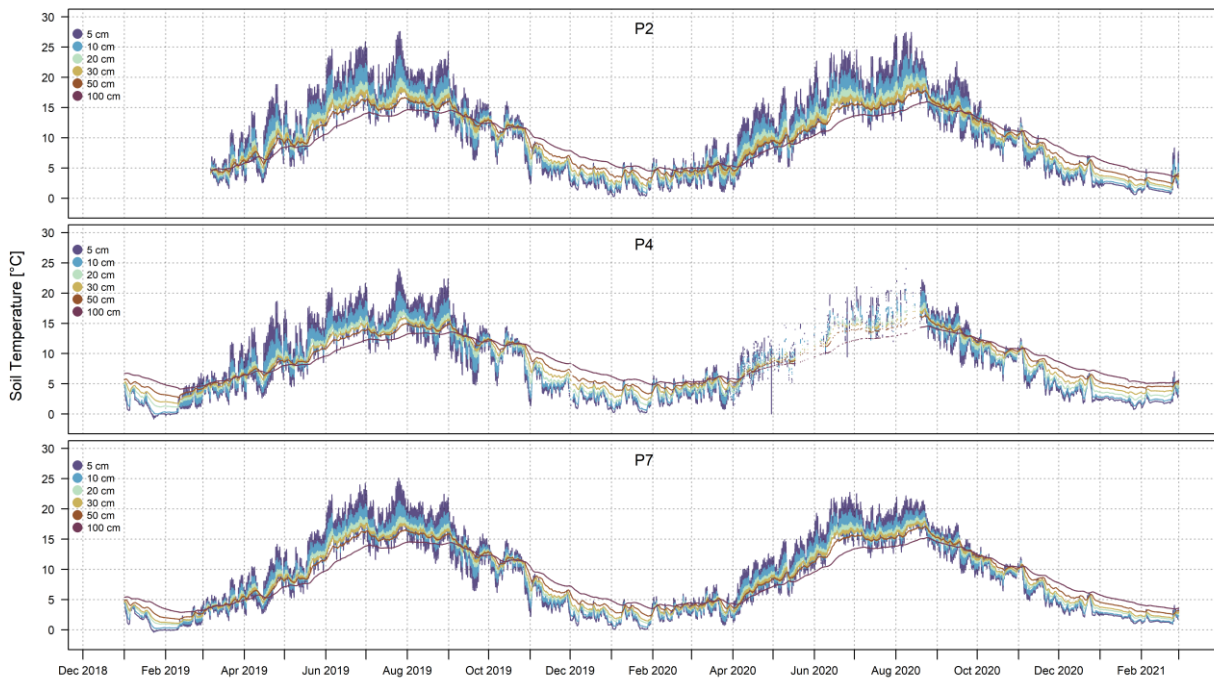


164

165 **Figure 4: Time series of hourly-soil water content data. The plots were made using the data set as it appears in the online archive.**
 166 **The data are plotted using a scientific colour scale from Cramer (2018) chosen according to the principles described in Cramer et**
 167 **al. (2020).**

168 **3.2 Soil temperature**

169 The stations P2, P4 and P6-P7 are instrumented with one Th3-s soil temperature profile probe (formerly UMS GmbH, Munich,
170 Germany) each, located nearby the instrumented soil profiles (Fig. 2) and connected via SDI-12 to the same data loggers and
171 power supply. The probes consist of six temperature sensors cased inside a tube made of glass-fibre fiber reinforced plastic and
172 placed at the fixed depths of 5, 10, 20, 30, 50 and 100 cm. Soil temperature is measured at the same times as the TDR traces.
173 The measured data are shown in Fig. 5. The influence of the geographical exposure of the slopes is particularly evident, e.g.
174 overall higher temperature and stronger dynamics for the south-exposed slopes compared to the other areas, as well as the
175 strongest dynamics near the surface compared to the deepest sensors. For every temperature profile, the soil temperature values
176 corresponding to the depths of the TDR profiles within the same cluster (i.e., the same topographic unit, namely Northern
177 slope, valley bottom and Southern slope) are calculated based on a linear interpolation and used for calculating the temperature
178 correction of the TDR measured soil water content values from the TDR traces according to Kaatz (1989). By doing this, we
179 assume that i) the soil temperature changes linearly with depth between the observations at 5, 10, 20, 30, 50 and 100 cm,
180 regardless of material properties changes in-between, and ii) the soil temperature measured at each of the three plots (i.e., P2,
181 P4 and P7) is representative for the cluster (i.e., cluster North consisting of P1, P2 and P3, measured at P2; cluster Valley
182 consisting of P4 and P5, measured at P4; cluster South consisting of P6, P7 and P8, measured at P7).

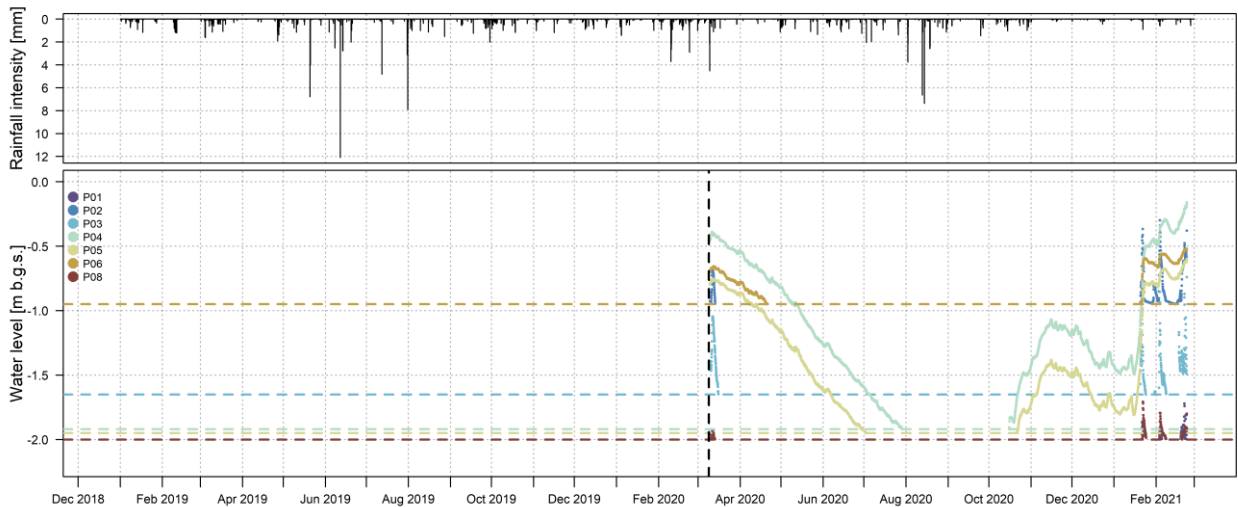


183

184 **Figure 5: Time series of hourly soil temperature data.** The plots were made using the data set as it appears in the online archive. The
185 data are plotted using a scientific colour scale from Crameri (2018) chosen according to the principles described in Crameri et al.
186 (2020).

187 3.3 Groundwater Water level

188 Every station of the *STH-net* is equipped with a monitoring well consisting of a LDPE (i.e, low-density polyethylene) tube
189 drilled to the maximum depth of 2 m and ~~screened in the depth interval 1–2 m~~ instrumented with levellogger LTC (Solinst,
190 Ontario, Canada), model 3001- M10. Due to an initial malfunctioning of the ~~piezometers~~sensors, only the data measured since
191 March 9th, 2020 are available ~~(not displayed)~~. In contrast to the other measurements of the data set presented here, the water
192 level data are downloaded manually. Figure 6 shows the time series of the water level data and reports the maximum depth for
193 every well. Seasonal dynamics of the groundwater level are evident for the wells in the valley bottom (P4 and P5) and for P6,
194 located next to the creek. The wells on the slopes (P1, P2, P3, P7 and P8) stay dry for most of the monitored period and only
195 show quick rises and recessions of the water level in the winter and spring season.

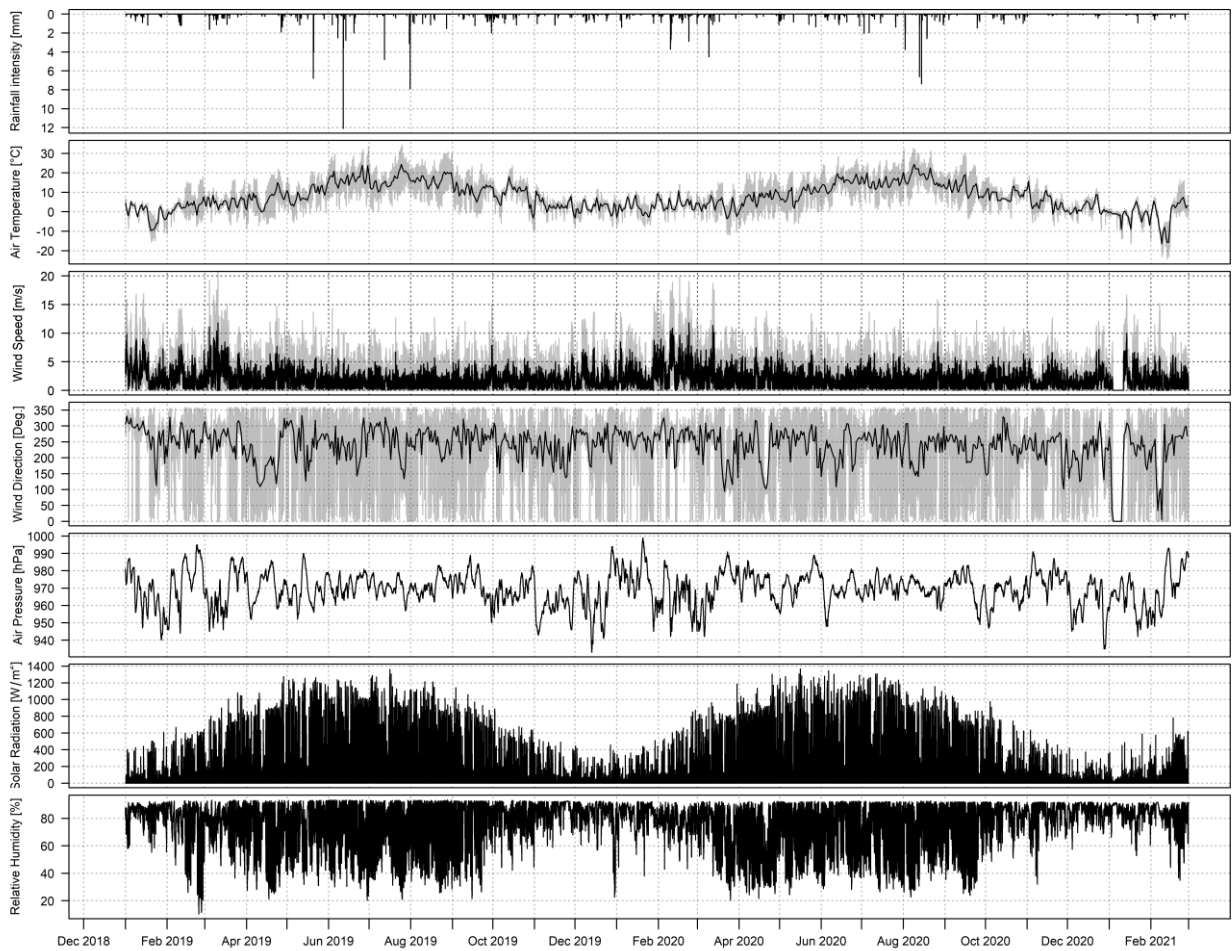


196

197 Figure 6: Time series of water level data. The plots were made using the data set as it appears in the online archive. The dashed
198 vertical line indicates the start of the measurements (March 9th, 2020). The dashed horizontal lines indicate the depth of the wells.
199 The data are plotted using a scientific colour scale from Crameri (2018) chosen according to the principles described in Crameri et
200 al. (2020).

201 3.4 Meteorological data

202 In the central part of the Schäfertal Hillslope site (Fig. 1), a WXT 520 weather station (Vaisala Oyj, Laskutus, Finland)
203 equipped with a CMP3-L pyranometer (Kipp & Zonen, Delft, Netherlands) installed at the height of 2 m measures the wind
204 vector, air temperature and pressure, relative humidity, liquid precipitation, hail and solar radiation. The system is fully
205 integrated with the data logger of the central monitoring station and the meteorological variables are measured at the same
206 times as the TDR and soil temperature profile probes. Fig. 6-7 shows the hourly time series of ~~rainfall intensity, air temperature~~
207 ~~and solar radiation~~ the meteorological variables.

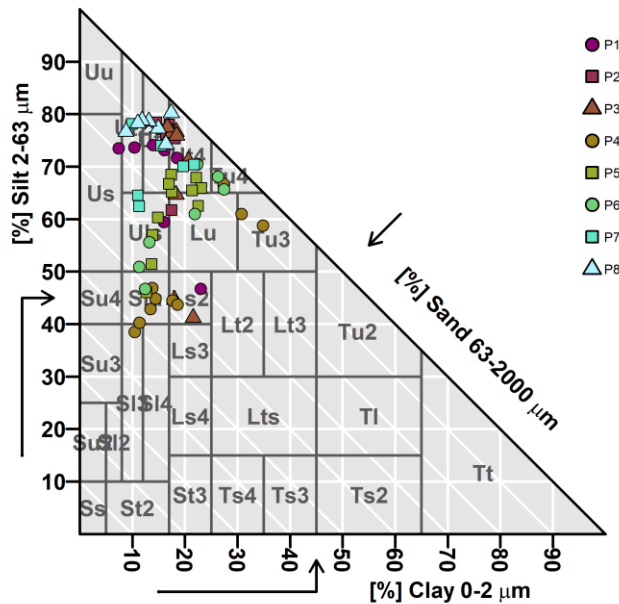


208

209 **Figure 76:** Time series of all the **most relevant** meteorological variables measured at the *Schäfertal Hillslope* site. The plots were
 210 made using the data set as it appears in the online archive. The black line in the second, third and fourth plots shows the daily
 211 average temperature, the average wind speed and the daily average wind direction, respectively while all other data are in **hourly**
 212 10-min time steps. **The plots were made using the hourly data set as it appears in the online archive.**

213 3.5 Soil properties

214 During the installation of the STH-net, one bulk soil sample and one volumetric soil sample were collected at every soil pit at
 215 the same depth as each of the TDR probes were installed. From the bulk samples, the percentage of sand, silt and clay in the
 216 fine earth fraction was determined in the laboratory using the pipette method. The volumetric soil samples were collected with
 217 a stainless stain ring and used for the soil porosity and bulk density estimation. Fig. 6-8 shows the classification of the soil
 218 samples according to the German soil textural classes (Ad-hoc-AG Boden, 2005), considered suitable for the soil
 219 parameterization for physically-based hydrological modelling (Bormann, 2007).



220

221 **Figure 87:** Soil textural classification according to the German *Bodenkundliche Kartieranleitung* (Ad-hoc-AG Boden, 2005) grouped
 222 by soil profiles (P1 to P8). *Ss*: pure sand; *Su2*: slightly silty sand; *Sl2*: slightly loamy sand; *Sl3*: medium loamy sand; *St2*: slightly
 223 clayey sand; *Su3*: medium silty sand; *Su4*: highly silty sand; *Slu*: loamy silty sand; *Sl4*: highly loamy sand; *St3*: medium clayey sand;
 224 *Ls2*: slightly sandy loam *Ls3*: medium sandy loam; *Ls4*: highly sandy loam; *Lt2*: slightly clayey loam; *Lts*: clayey sandy loam; *Ts4*:
 225 highly sandy clay; *Ts3*: medium sandy clay; *Uu*: pure silt; *Us*: sandy silt; *Ut2*: slightly clayey silt; *Ut3*: medium clayey silt; *Uls*: loamy
 226 sandy silt; *Ut4*: highly clayey silt; *Lu*: silty loam; *Lt3*: medium clayey loam; *Tu3*: medium silty clay; *Ts2*: slightly sandy clay; *Tu4*:
 227 highly silty clay; *Tu2*: slightly silty clay; *Tl*: loamy clay; *Tt*: pure clay. The figure was created in RStudio with the package “The Soil
 228 Texture Wizard” (<https://CRAN.R-project.org/package=soiltexture>) by Julien Moeys. The data are plotted using a scientific colour
 229 scale from Crameri (2018) chosen according to the principles described in Crameri et al. (2020).

230 4 Uncertainties and data usability

231 [For the estimation of soil water content using a composite dielectric approach, some physical parameters must be known.](#)
 232 [These are primarily temperature, porosity and the dielectric number of the solid matrix \(\$\epsilon_{soil}\$ \). Among them, soil temperature](#)
 233 [plays the major role in determining the global uncertainty. As part of the *STH-net*, soil temperature is measured in situ at the](#)
 234 [same time as the TDR waveforms, which enables an accurate temperature correction. The soil porosity was estimated for every](#)
 235 [sampling point from undisturbed soil cores and introduces an uncertainty. For \$\epsilon_{soil}\$ we have chosen the value of 4.6,](#)
 236 [corresponding to the dielectric permittivity of quartz. This value was chosen arbitrarily hence introduces an uncertainty. For](#)
 237 [a more extensive discussion about the uncertainty of the soil water content estimation as due to the single parameters we refer](#)
 238 [to Roth et al. \(1990\). For the data set presented here, we estimated the uncertainty of the calculated soil water content using](#)
 239 [the CRIM formula by varying the values of \$\epsilon_{soil}\$ and porosity between 4 and 6 and between 0.3 and 0.5, respectively \(similar](#)

240 [to Wollschläger et al., 2010](#)). We obtained values $< \pm 0.03 \text{ m}^3/\text{m}^3$ as largest uncertainty of the soil water content estimation.
241 [This information is reported in Table 1 along with the measurement range, accuracy and resolution of the other variables](#)
242 [provided within the data set described in this article](#).
243 [Rain gauges may misestimate the rainfall rate under certain circumstances, especially when rainfall events are associated to](#)
244 [strong wind. The experiment described in Basara et al. \(2009\) shows that a sensor similar to the one installed at the *Schäfertal*](#)
245 [Hillslope site overestimates the rainfall intensity in an urban environment. The rainfall rate data presented in this article were](#)
246 [compared to those of several other rain gauges \(data from partner research institute, not available here\) located ca. 100 m away](#)
247 [from the site. The rainfall intensity values measured by our sensor do not underestimate the rainfall rate values nor completely](#)
248 [miss rainfall events. With our data set, we make the measured data available to any interested scientists along with all relevant](#)
249 [site information and let them the choice about eventual compensation measures to be applied. The correction function proposed](#)
250 [by Richter \(1995\) is commonly used for studies conducted in Central Germany to account for the possible wind-induced](#)
251 [underestimation of the rainfall intensity](#).
252 [Until a few years ago, the Schäfertal catchment used to be affected by significant snowfall, with major snowmelt events](#)
253 [occurring between January and April, whose effects on the hydrological processes are described, e.g., in Ollesch et al. \(2005\).](#)
254 [In the last years, however, no significant snowfall events were observed. The last winter period \(December 2020 to February](#)
255 [2021\), instead, was characterized by exceptionally intense snowfall \(with a maximum of ca. 45 cm on February 8th, 2021\) that](#)
256 [accumulated and persisted. Unfortunately, the technical infrastructure currently available at the site does not allow a](#)
257 [meaningful estimation of the snow height and distribution during the monitoring period, hence the snowfall events are not](#)
258 [recorded by the weather station in use \(see Fig. 7\). Because of this, the snow contribution to the water balance needs to be](#)
259 [derived from the meteorological and soil temperature data available](#).
260 [Overall, 9.3 % of the soil water content data and 7.6 % of the soil temperature data are missing \(particularly until March 2019](#)
261 [for the station North and between April and August 2020 for the station Valley\) due to various technical failures](#).
262

263 **Table 1: Measurement range, accuracy and resolution of the measurement devices described in Section 3.**

	<u>Measurement range</u>	<u>Accuracy</u>	<u>Resolution</u>
<u>STH-net station</u>			
<u>Soil water content¹</u>	<u>0 to 1 m³/m³</u>	<u>< ±0.03 m³/m³</u>	<u>-</u>
<u>Soil temperature²</u>	<u>-20°C to +50°C</u>	<u>± 0,1°C</u>	<u>0,034°C</u>
<u>Water level³</u>	<u>0 to 50°C (Barologger 5: -10 to +50°C), FS = 10 m</u>	<u>± 0.5 cm</u>	<u>0.0006% FS</u>
<u>Weather station</u>			
<u>Barometric Pressure⁴</u>	<u>600 to 1100 hPa</u>	<u>±0.5 hPa at 0 to +30 °C</u> <u>±1 hPa at -52 to +60 °C</u>	<u>0.1 hPa, 10 Pa, 0.001 bar, 0.1 mmHg, 0.01 inHg</u>
<u>Air Temperature⁴</u>	<u>-52 to +60 °C</u>	<u>±0.3 °C</u>	<u>0.1 °C</u>
<u>Wind speed⁴</u>	<u>0 to 60 m/s</u>	<u>±3 % at 10 m/s</u>	<u>0.1 m/s</u>
<u>Wind direction⁴</u>	<u>0 to 360° azimuth</u>	<u>±3.0°</u>	<u>1°</u>
<u>Relative Humidity⁴</u>	<u>0 to 100 % RH</u>	<u>±3 %RH at 0 to 90 %RH</u> <u>±5 %RH at 90 to 100 %RH</u>	<u>0.1 %RH</u>
<u>Rainfall intensity⁴</u>	<u>0 to 200 mm/h (broader range with reduced accuracy)</u>	<u>Daily accumulation: better than 5 %, weather dependent</u>	<u>0.01 mm</u>
<u>Hail⁴</u>	<u>n.a.</u>	<u>n.a</u>	<u>0.1 hit/cm²</u>
<u>Solar radiation⁵</u>	<u>Maximum solar irradiance: 2000 W/m²</u>	<u>±5 %</u>	<u>< ±5 W/m²</u>

264 ¹ custom-made TDR probes (Helmholtz Centre for Environmental Research GmbH – UFZ, Leipzig, Germany)265 ² Th3-s soil temperature profile probe (formerly UMS GmbH, Munich, Germany). Source: <https://www.google.com/url?sa=t&rct=j&q=&esrc=s&source=web&cd=&ved=2ahUKEwjQjpTu4bvUAhWm4YUKHTKhCsUQFjABegQIARAC&url=http%3A%2F%2Ffcnyhome.cafe24.com%2Fpdf%2FTh3sManual.pdf&usq=AOvVaw1JN8EI6XoJ6F3LyJw9PnnK> (accessed Apr 13th, 2021).266 ³ 3001-M10 levelogger LTC (Solinst, Ontario, Canada). Source: <https://www.solinst.com/products/data/3001-ltc.pdf> (accessed Apr 13th, 2021).267 ⁴ WXT 520 weather station (Vaisala Oyj, Laskutus, Finland). Source: <https://www.vaisala.com/en/file/9411/download?token=DOb1ETJK> (accessed Apr 13th, 2021).268 ⁵ CMP3-L pyranometer (Kipp & Zonen, Delft, Netherlands). Source: <https://www.kippzonen.com/Product/11/CMP3-Pyranometer> (accessed Apr 13th, 2021).275 **4.5 Data management**

276 The *STH-net* data stored by the three data loggers are accessed and downloaded remotely using the software *Loggernet*

277 (Campbell Scientific Inc., Logan, UT, United States). The only exception are the water level data, which are manually

278 downloaded. The data files are regularly quality checked and ~~processed using a custom made code running on RStudio~~

279 ~~(RStudio Team, 2019). The original files are averaged to hourly values and~~ uploaded to the EUDAT record *STH-net*

280 ~~(<https://b2share.eudat.eu/records/e2a2135bb1634a97abcedf8a461e0909>~~[https://b2share.eudat.eu/records/82818db7be054f5eb](https://b2share.eudat.eu/records/82818db7be054f5eb921d386a0bcaa74)

281 [921d386a0bcaa74](https://b2share.eudat.eu/records/82818db7be054f5eb921d386a0bcaa74)), where they remain available for download. ~~For soil water content data only, the full resolution data were~~

282 denoised using a moving average smoothing (width of 12 hours) prior to the hourly aggregation. This procedure was compared
283 to others and proved to be effective in removing the measurement noise while keeping the dynamic component of the signal.
284

285 **5-6 Data sets**

286 The *STH-net* data are archived as separate text files for the different data types: soil water content, soil temperature, [water level](#)
287 and meteorological variables. Furthermore, the geographic coordinates of the measurement locations and the soil information
288 are available for download. The time series data start from January 1st, 2019 and continue with hourly time steps until the most
289 recent update. At the time of the manuscript submission, the latest entry refers to ~~September 30th, 2020~~ [February 28th, 2021](#).
290 [The water level data are available with a 2-hours resolution and covers the time period between March 6th, 2020 and February,](#)
291 [23rd, 2021. All the data published in the online archive \(DOI 10.23728/b2share.82818db7be054f5eb921d386a0bcaa74\) will](#)
292 [be updated approximately on a 3-months basis.](#)

293 **6-7 Data availability**

294 The *STH-net* data are available under a dynamic identifier DOI
295 ~~10.23728/b2share.e2a2135bb1634a97abcedf8a461e0909~~ [10.23728/b2share.82818db7be054f5eb921d386a0bcaa74](#) (Martini et
296 al., 2020) at the time of the manuscript submission (from there, all future versions of the archive can be easily accessed) under
297 the Creative Commons Attribution license (CC-BY 4.0).

298 **Author contribution**

299 Edoardo Martini: conceptualization, data curation, formal analysis, funding acquisition, investigation, methodology,
300 visualization, writing – original draft preparation, writing – review & editing.

301 [Matteo Bauckholt: data curation.](#)

302 Simon Kögler: conceptualization, data curation, methodology.

303 Manuel Kreck: data curation, methodology, writing – review & editing.

304 Kurt Roth: conceptualization, resources, writing – review & editing

305 Ulrike Werban: conceptualization, funding acquisition, resources, writing – review & editing

306 Ute Wollschläger: conceptualization, writing – review & editing

307 Steffen Zacharias: conceptualization, funding acquisition, resources, writing – review & editing

308 **Competing interests**

309 The authors declare that they have no conflict of interest.

310 **Acknowledgments**

311 The installation and operation of Schäfertal Hillslope site research infrastructure was funded and supported by the Terrestrial
312 Environmental Observatories (TERENO), which is a joint collaboration program involving several Helmholtz Research
313 Centres in Germany, and the TERENO observatory Harz/Central German Lowland operated by the UFZ Helmholtz Centre
314 for Environmental Research is gratefully acknowledged for providing access to the *Schäfertal Hillslope* site and to the *STH-*
315 *net* data. Edoardo Martini received funding from the German Research Foundation (DFG) through the research grant MA
316 7936/1-1.

317 **References**

- 318 Ad-hoc-Arbeitsgruppe Boden: Bodenkundliche Kartieranleitung, Bundesanstalt für Geowissenschaften und Rohstoffe in
319 Zusammenarbeit mit den Staatlichen Geologischen Diensten, 5. Aufl., 438p., Hannover, ISBN 978-3-510-95920-4, 2005.
- 320 ~~Anderson, S.P., Bales, R.C., and Duffy, C.J.: Critical Zone Observatories: Building a network to advance interdisciplinary~~
321 ~~study of Earth surface processes, *Mineralogical Magazine*, 72(1), 7–10, <https://doi.org/10.1180/minmag.2008.072.1.7>, 2008.~~
- 322 Bauser, H.H., Jaumann, S., Berg, D., and Roth, K.: EnKF with closed-eye period - Towards a consistent aggregation of
323 information in soil hydrology, *Hydrol. Earth Syst. Sci.*, 20, 4999–5014. <https://doi.org/10.5194/hess-20-4999-2016>, 2016.
- 324 Bauser, H.H., Riedel, L., Berg, D., Troch, P.A., and Roth, K.: Challenges with effective representations of heterogeneity in
325 soil hydrology based on local water content measurements. *Vadose Zone Journal*, 19:e20040,
326 <https://doi.org/10.1002/vzj2.20040>, 2020.
- 327 Blöschl, G., Bierkens, M. F. P., Chambel, A., et al.: Twenty-three Unsolved Problems in Hydrology (UPH) – a community
328 perspective, *Hydrolog. Sci. J.*, 64, 1141–1158, <https://doi.org/10.1080/02626667.2019.1620507>, 2019.
- 329 Borchardt, D.: Geoökologische Erkundung und hydrologische Analyse von Kleinzugsgebieten des unteren
330 Mittelgebirgsbereichs, dargestellt am Beispiel der oberen Selke, Harz, *Petermanns Geogr. Mitteil.*, 82, 251–262, 1982.
- 331 Botto, A., Belluco, E., and Camporese, M.: Multi-source data assimilation for physically based hydrological modeling of an
332 experimental hillslope, *Hydrol. Earth Syst. Sci.*, 22, 4251–4266, <https://doi.org/10.5194/hess-22-4251-2018>, 2018.
- 333 Bormann, H.: Analysis of the suitability of the German soil texture classification for the regional scale application of physical
334 based hydrological model, *Adv. Geosci.*, 11, 7–13, <https://doi.org/10.5194/adgeo-11-7-2007>, 2007.
- 335 Bronstert, A.: Capabilities and limitations of detailed hillslope hydrological modelling, *Hydrol. Process.*, 13: 21–48.
336 [doi:10.1002/\(SICI\)1099-1085\(199901\)13:1<21::AID-HYP702>3.0.CO;2-4](https://doi.org/10.1002/(SICI)1099-1085(199901)13:1<21::AID-HYP702>3.0.CO;2-4), 1999.

337 Clark, M.P., Bierkens, M.F.P., Samaniego, L., Woods, R.A., Uijlenhoet, R., Bennett, K.E., Pauwels, V.R.N., Cai, X., Wood,
338 A.W., and Peters-Lidard, C.D.: The evolution of process-based hydrologic models: historical challenges and the collective
339 quest for physical realism, *Hydrol. Earth Syst. Sci.*, 21, 3427–3440, <https://doi.org/10.5194/hess-21-3427-2017>, 2017.

340 Crameri, F.: Scientific colour maps, Zenodo, <http://doi.org/10.5281/zenodo.1243862>, 2018.

341 Crameri, F., Shephard, G.E., and Heron, P.J.: The misuse of colour in science communication, *Nature Communications*, 11,
342 5444, doi:10.1038/s41467-020-19160-7, 2020.

343 Fan, Y., Clark, M., Lawrence, D. M., Swenson, S., Band, L. E., Brantley, S. L., et al.: Hillslope hydrology in global -change
344 research and Earth system modeling, *Water Resources Research*, 55, 1737–1772, <https://doi.org/10.1029/2018WR023903>,
345 2019.

346 Graeff, T., Zehe, E., Reusser, D., Lück, E., Schröder, B., Wenk, G., John, H., and Bronstert, A.: Process identification through
347 rejection of model structures in a mid-mountainous rural catchment: observations of rainfall–runoff response, geophysical
348 conditions and model inter-comparison, *Hydrol. Process.*, 23: 702–718. doi:10.1002/hyp.7171, 2009.

349 ~~Guo, L. and Lin, H.: Critical zone research and observatories: Current status and future perspectives, *Vadose Zone J.* 15(9),
350 doi:10.2136/vzj2016.06.0050, 2016.~~

351 [Kaatze, U.: Complex permittivity of water as a function of frequency and temperature, *J. Chem. Eng. Data* 1989, 34, 4, 371–
352 374, <https://doi.org/10.1021/je00058a001>, 1989.](https://doi.org/10.1021/je00058a001)

353 [IUSS Working Group WRB: World Reference Base for Soil Resources 2014, Update 2015. World Soil Resources Reports
354 106, FAO, Rome. ISBN 978-92-5-108369-7, 2015.](https://doi.org/10.1021/je00058a001)

355 Martini, E., Wollschläger, U., Kögler, S., Behrens, T., Dietrich, P., Reinstorf, F., Schmidt, K., Weiler, M., Werban, U., and
356 Zacharias, S.: Spatial and temporal dynamics of hillslope-scale soil moisture patterns: characteristic states and transition
357 mechanisms, *Vadose Zone J.*, 14, doi:10.2136/vzj2014.10.0150, 2015.

358 Martini, E., Werban, U., Zacharias, S., Pohle, M., Dietrich, P., and Wollschläger, U.: Repeated electromagnetic induction
359 measurements for mapping soil moisture at the field scale: validation with data from a wireless soil moisture monitoring
360 network, *Hydrol. Earth Syst. Sci.*, 21, 495–513, <https://doi.org/10.5194/hess-21-495-2017>, 2017.

361 Martini, E., Wollschläger, U., Musolff, A., Werban, U., and Zacharias, S.: Principal component analysis of the spatiotemporal
362 pattern of soil moisture and apparent electrical conductivity, *Vadose Zone J.*, 16(10), doi:10.2136/vzj2016.12.0129, 2017.

363 Martini, E., Kögler, S., Kreck, M., Werban, U., Wollschläger, U., Zacharias, S.: STH-net, EUDAT,
364 <https://b2share.eudat.eu/records/e2a2135bb1634a97abcedf8a461e0909>[https://b2share.eudat.eu/records/82818db7be054f5e
365 b921d386a0bcaa74](https://b2share.eudat.eu/records/82818db7be054f5eb921d386a0bcaa74), 2020.

366 Ollesch, G., Sukhanovski, Y., Kistner, I., Rode, M., and Meissner, R.: Characterization and modelling of the spatial
367 heterogeneity of snowmelt erosion, *Earth Surf. Proc. Land.*, 30, 197–211, doi:10.1002/esp.1175, 2005.

368 Reinstorf, F.: Schäfertal, Harz Mountains, Germany. Poster, in: Status and Perspectives of Hydrology in Small Basins, Results
369 and recommendations of the International Workshop in Goslar-Hahnenklee, Germany 2009, and Inventory of Small
370 Hydrological Research Basins, 30 March–2 April 2009, Goslar-Hahnenklee, Germany, edited by: Schumann, S., Schmalz,

371 B., Meesenburg, H., and Schröder, U., available at:
372 [https://www.google.com/url?sa=t&rct=j&q=&esrc=s&source=web&cd=&ved=2ahUKewjQluqSIMjsAhUOecAKHTnICqsQFjAAegQIAhAC&url=https%3A%2F%2Fwaterandchange.org%2Fwp-](https://www.google.com/url?sa=t&rct=j&q=&esrc=s&source=web&cd=&ved=2ahUKewjQluqSIMjsAhUOecAKHTnICqsQFjAAegQIAhAC&url=https%3A%2F%2Fwaterandchange.org%2Fwp-content%2Fuploads%2F2017%2F04%2FHeft10_en.pdf&usg=AOvVaw2o4w_VX74jGiquRs3KaYVR)
373 [content%2Fuploads%2F2017%2F04%2FHeft10_en.pdf&usg=AOvVaw2o4w_VX74jGiquRs3KaYVR](https://www.google.com/url?sa=t&rct=j&q=&esrc=s&source=web&cd=&ved=2ahUKewjQluqSIMjsAhUOecAKHTnICqsQFjAAegQIAhAC&url=https%3A%2F%2Fwaterandchange.org%2Fwp-content%2Fuploads%2F2017%2F04%2FHeft10_en.pdf&usg=AOvVaw2o4w_VX74jGiquRs3KaYVR) (last access: 22
374 October 2020), 2010.

375
376 [Richter, D.: Ergebnisse methodischer Untersuchungen zur Korrektur des systematischen Meßfehlers des Hellmann-](#)
377 [Niederschlagsmessers, Berichte des Deutschen Wetterdienstes 194, Deutscher Wetterdienst, Offenbach am Main, ISBN:](#)
378 [3881483098, http://nbn-resolving.de/urn:nbn:de:101:1-201601274368, in German, 1995](#)

379 Roth, K., Schulin, R., Flühler, H., and Attinger, W.: Calibration of time domain reflectometry for water content measurement
380 using a composite dielectric approach, *Water Resour. Res.*, 26, 2267–2273, doi:10.1029/WR026i010p02267, 1990.

381 RStudio Team: RStudio: Integrated Development for R. RStudio, Inc., Boston, MA URL <http://www.rstudio.com/>, 2019.

382 Schröter, I., Paasche, H., Dietrich, P., and Wollaschläger, U.: Estimation of catchment-scale soil moisture patterns based on
383 terrain data and sparse TDR measurements using a Fuzzy C-Means clustering approach, *Vadose Zone J.*, 14,
384 doi:10.2136/vzj2015.01.0008, 2015.

385 United Nations: World Soil Day and International Year of Soils: A/RES/68/232, 2014.

386 Vogel, H.-J.: Scale issues in soil hydrology, *Vadose Zone J.*, 18(1). <https://doi.org/10.2136/vzj2019.01.0001>, 2019.

387 Vrugt, J.A., Stauffer, P.H., Wöhling, T., Robinson, B.A., and Vesselinov, V.V.: Inverse modeling of subsurface flow and
388 transport properties: A review with new developments, *Vadose Zone Journal*, 7, 843–864.
389 <https://doi.org/10.2136/vzj2007.0078>, 2008.

390 Vereecken, H., Huisman, J. A., Hendricks Franssen, H. J., Brüggemann, N., Bogaen, H. R., Kollet, S., Javaux, M., van der
391 Kruk, J., and Vanderborght, J.: Soil hydrology: Recent methodological advances, challenges, and perspectives. *Water*
392 *Resources Research*, <https://doi.org/10.1002/2014WR016852>, 2015.

393 Vereecken, H., Schnepf, A., Hopmans, J. W., Javaux, M., Or, D., Roose, T., J. Vanderborght, Young, M. H., Amelung, W.,
394 Aitkenhead, M., Allison, S. D., Assouline, S., Baveye, P., Berli, M., Brüggemann, N., Finke, P., Flury, M., Gaiser, T., Govers,
395 G., Ghezzehei, T., Hallett, P., Hendricks Franssen, H. J., Heppell, J., Horn, J., Huisman, J. A., Jacques, D., Jonard, F., Kollet,
396 S., Lafolie, F., Lamorski, K., Leitner, D., McBratney, A., Minasny, B., Montzka, C., Nowak, W., Pachepsky, Y., Padarian,
397 J., Romano, N., Roth, K., Rothfuss, Y., Rowe, E. C., Schwen, A., Šimůnek, J., Tiktak, A., van Dam, J., van der Zee, S. E. A.
398 T. M., Vogel, H.-J., Vrugt, J. A., Wöhling, T., & Young, I. M. (2016). Modeling Soil Processes: Review, Key challenges
399 and New Perspectives. *Vadose Zone Journal*, 15(5), 1–57, <https://doi.org/10.2136/vzj2015.09.0131>.

400 Wollaschläger, U., Pfaff, T., and Roth, K.: Field-scale apparent hydraulic parameterisation obtained from TDR time series and
401 inverse modelling, *Hydrol. Earth Syst. Sci.*, 13, 1953–1966, doi:10.5194/hess-13-1953-2009, 2009.

402 [Wollaschläger, U., Gerhards, H., Yu, Q., and Roth, K.: Multi-channel ground-penetrating radar to explore spatial variations in](#)
403 [thaw depth and moisture content in the active layer of a permafrost site, *The Cryosphere* 4.3: 269-283, 2010.](#)

404 Wollschläger, U., Attinger, S., Borchardt, D., Brauns, M., Cuntz, M., Dietrich, P., Fleckenstein, J.H., Friese, K., Friesen, J.,
405 Harpke, A., Hildebrandt, A., Jäckel, G., Kamjunke, N., Knöller, K., Kögler, S., Kolditz, O., Krieg, R., Kumar, R., Lausch,
406 A., Liess, M., Marx, A., Merz, R., Mueller, C., Musolff, A., Norf, H., Oswald, S.E., Reibmann, C., Reinstorf, F., Rode, M.,
407 Rink, K., Rinke, K., Samaniego, L., Vieweg, M., Vogel, H.-J., Weitere, M., Werban, U., Zink, M., and Zacharias, S. : The
408 Bode Hydrological Observatory: A platform for integrated, interdisciplinary hydro-ecological research within the TERENO
409 Harz/Central German Lowland Observatory, *Env. Earth Sci.*, 76:29, doi:10.1007/s12665-016-6327-5, 2017.

410 Zacharias, S., Boga, H., Samaniego, L., Mauder, M., Fuß, R., Pütz, T., Frenzel, M., Schwank, M., Baessler, C., Butterbach-
411 Bahl, K., Bens, O., Borg, E., Brauer, A., Dietrich, P., Hajnsek, I., Helle, G., Kiese, R., Kunstmann, H., Klotz, S., Munch, J.
412 C., Papen, H., Priesack, E., Schmid, H. P., Steinbrecher, R., Rosenbaum, U., Teutsch, G., and Vereecken, H.: A network of
413 terrestrial environmental observatories in Germany, *Vadose Zone J.*, 10, 955–973, doi:10.2136/vzj2010.0139, 2011.

414